Please cite this article in press as: Spokoini et al., Confinement to Organelle-Associated Inclusion Structures Mediates Asymmetric Inheritance of Aggregated Protein in Budding Yeast, Cell Reports (2012), http://dx.doi.org/10.1016/j.celrep.2012.08.024

Cell Reports
Report

Confinement to Organelle-Associated Inclusion Structures Mediates Asymmetric Inheritance of Aggregated Protein in Budding Yeast

Rachel Spokoini,[1] Ofer Moldavski,[2] Yaakov Nahmias,[1] Jeremy L. England,[3] Maya Schuldiner,[2] and Daniel Kaganovich[1,*]
[1]Department of Cell and Developmental Biology, Alexander Silberman Institute of Life Sciences, Hebrew University of Jerusalem, Jerusalem 91904, Israel
[2]Department of Molecular Genetics, Weizmann Institute of Science, Rehovot 76100, Israel
[3]Department of Physics, Massachusetts Institute of Technology, Cambridge, MA 02139, USA
*Correspondence: dan@cc.huji.ac.il
http://dx.doi.org/10.1016/j.celrep.2012.08.024

SUMMARY

The division of the *S. cerevisiae* budding yeast, which produces one mother cell and one daughter cell, is asymmetric with respect to aging. Remarkably, the asymmetry of yeast aging coincides with asymmetric inheritance of damaged and aggregated proteins by the mother cell. Here, we show that misfolded proteins are retained in the mother cell by being sequestered in juxtanuclear quality control compartment (JUNQ) and insoluble protein deposit (IPOD) inclusions, which are attached to organelles. Upon exposure to stress, misfolded proteins accumulate in stress foci that must be disaggregated by Hsp104 in order to be degraded or processed to JUNQ and IPOD. Cells that fail to deliver aggregates to an inclusion pass on aggregates to subsequent generations.

INTRODUCTION

Protein aggregation has the potential to cause toxicity in any cell where it is not properly managed. Cells have therefore developed a multilayered quality control machinery to avoid accumulating aggregates or to sequester aggregating proteins in a way that reduces their harmful impact (Rujano et al., 2006; Tyedmers et al., 2010a). The necessity for quality control does not stop at the intracellular level: cell division is the cell's final opportunity to prevent aggregates from being inherited by the next generation. This intergenerational form of quality control has been termed spatial quality control (Nyström, 2011; Treusch et al., 2009).

In budding yeast, while the mother cell ages with each new budding event until it dies, the daughter cells are born with a new replicative life span clock. Although this phenomenon has been well documented (Delaney et al., 2011; Nyström, 2011; Treusch et al., 2009), we know little about the molecular events that cause either aging or aging-associated death. Likewise, it is unclear how daughter cells avoid inheriting the replicative aging state of the mother. In previous studies, it was noted that in budding yeast, the replicative aging of a mother cell corresponds to the asymmetric inheritance of damaged proteins, as visualized either with an antibody against carbonylated proteins that were chemically modified with dinitrophenylhydrazine (Erjavec et al., 2007) or a green fluorescent protein (GFP)-tagged aggregate-binder, like the Hsp104 chaperone (Aguilaniu et al., 2003; Erjavec et al., 2007; Henderson and Gottschling, 2008; Shorter and Lindquist, 2006; Winkler et al., 2012). Yeast that were deleted for the Sir2 deacetylase (Delaney et al., 2011) or Hsp104 chaperone had a shortened life span corresponding to contamination of daughter cells with damaged proteins during division (Erjavec and Nyström, 2007).

The mechanism through which mother cells asymmetrically inherit aggregates has remained controversial. One study (Liu et al., 2010) demonstrated that the Sir2 deletion resulted in a defect in the actin cytoskeleton. Actin, in turn, was shown to be required for preventing Hsp104-colocalizing puncta from entering the nascent bud via a mechanism mediated by the "polarisome" complex anchoring actin cables. A recent direct response to this study (Zhou et al., 2011) tracked the motions of Hsp104-bound protein aggregates in live yeast cells. Since the trajectories they observed were quite jagged, it was concluded that the aggregates' movements should be modeled as an ad hoc stochastic process that would produce the experimentally observed distribution of time dependence for mean-square displacement as a function of time. On this basis, the study argued that the curious phenomenon of asymmetric inheritance of aggregates upon cell division is the result of just such a random diffusion process taking place in boundary conditions determined by the shape of budding yeast.

Here, we argue against the stochastic model of Zhou et al. (2011) and in favor of an alternative mechanism for keeping nascent buds free of aggregates. By carefully tracking model proteins from misfolding and aggregation in the mother cell until after cell division, we have determined that these proteins initially aggregate in small amorphous foci that we call proteostatic stress foci, and subsequently become sequestered in inclusions. We show that those aggregates, which accumulate in inclusions, are uniformly retained in the mother cell during budding. When, on the other hand, deletion of Hsp104 is used to trap aggregates in stress foci, many of them can pass into the daughter cells and some are inherited by the second and third generation. Interestingly, the model aggregating proteins examined in this study appear to be sequestered in inclusions prior to the budding

Cell PRESS
Open ACCESS

event. The movement of inclusions between mother and bud, on the other hand, is constrained by their attachment to cellular organelles. We therefore suggest that confinement of aggregates in inclusions may be one of the general mechanisms for excluding them from nascent daughter cells.

RESULTS

Misfolded Protein Aggregates Can Form Proteostatic Stress Foci, Juxtanuclear Quality Control Compartment Inclusions, or Insoluble Protein Deposit Inclusions

In eukaryotes, aggregation prone proteins are partitioned between the juxtanuclear quality control compartment (JUNQ) and the insoluble protein deposit compartment (IPOD) (Tyedmers et al., 2010a; Figure 1A). Proteins that are ubiquitinated by the protein folding quality control machinery are delivered to the JUNQ (Figures 1B and S1A; Movie S1) where they are processed for degradation by the proteasome. Misfolded proteins that are not ubiquitinated are diverted to the IPOD where they are actively aggregated in a protective compartment (Figure 1C). IPODs are juxtavacuolar sites where Hsp104-GFP colocalizes with insoluble aggregates (Kaganovich et al., 2008; also Figures 1E and S1B).

In order to determine how asymmetric inheritance of aggregates in yeast is governed, we monitored the inheritance of two model aggregation-prone proteins (Kaganovich et al., 2008), misfolded von Hippel-Lindau protein (VHL) and Ubc9^{ts}, using high-resolution live-cell three-dimensional (3D) time lapse (four-dimensional [4D] imaging). von Hippel-Lindau protein and Ubc9^{ts} model misfolding events that frequently occur in yeast, namely the formation of aggregates from unassembled subunits of a heteroligomeric complex (VHL) or thermal denaturation (Ubc9^{ts}). When these proteins misfold and aggregate due to heat shock, they form proteostatic stress foci that colocalize with Hsp104 and are distinct from JUNQ and IPOD inclusions (Figures 1B, 1D, and 1E; Movie S3; data not shown for Ubc9^{ts}). Tracking these stress foci of VHL and Ubc9^{ts} with 4D imaging revealed that all of them dissolve on a time scale that is shorter than the yeast cell cycle (1–2 hr) (Kaganovich et al., 2008; Figure S2B) and are degraded in wild-type yeast (Kaganovich et al., 2008). Under mild stress and proteasome-inhibition conditions, misfolded proteins in the cytosol and in stress foci are processed into JUNQ and IPOD inclusions (Figure 1F; Movie S4). In cells where the misfolded protein is not ubiquitinated it is targeted directly to a single IPOD inclusion, without first forming stress foci (Figure 1C). Whereas the stress foci always colocalize with Hsp104, as does the IPOD, the JUNQ does not (Figures 1B, 1C, 1D, and S1A; Movies S1 and S2), though small amounts of Hsp104 can be detected in the JUNQ after prolonged severe stress (Kaganovich et al., 2008); D.K., unpublished data). We suggest, therefore, that previous studies that used tagged Hsp104 to detect aggregates usually observed stress foci and IPODs without distinguishing between them, but not JUNQ inclusions (Zhou et al., 2011).

JUNQ and IPOD Inclusions are Asymmetrically Inherited During Cell Division

Given that inclusion formation of VHL and Ubc9^{ts} aggregates preceded budding, we reasoned that inheritance of inclusions must be accounted for in order to explain asymmetric segregation of aggregates. Hence, we went on to examine the inheritance of the JUNQ and IPOD inclusions. Strikingly, both the JUNQ and the IPOD are invariably retained by the mother cell during budding (Figures 1G and 1H; Movies S5 and S6). We observed JUNQ and IPOD retention in several consecutive budding events of the same mother (Movies S5 and S6), suggesting that delivery to inclusions is a critical step in managing the asymmetric inheritance of aggregates.

Hsp104 is Required for Disaggregating Stress Foci

In order to test this model, we required a method of preventing delivery of aggregates to the inclusions. Although depolymerizing the actin cytoskeleton has been used to generate aggregate structures in the past (Specht et al., 2011), this approach disrupts the entire spatial organization of the cell, affects cell division, and therefore complicates the question of asymmetry during division. We reasoned that, since Hsp104 is observed in association with aggregates and the actin cytoskeleton (Liu et al., 2011) and since it is required for aggregate clearance (Kaganovich et al., 2008; Figure 2A), the disaggregase chaperone might also be required for the subsequent conversion of aggregates to inclusions. Interestingly, we observed that once proteins form stress foci upon mild heat shock, they require Hsp104 to be released from this state in order to undergo degradation or form inclusions (Figure 2A and data not shown). Indeed, when we heat shocked cells expressing VHL or Ubc9^{ts} in an Hsp104 deletion background, the stress foci phenotype persisted indefinitely, even after prolonged recovery at 25°C, and the misfolded proteins were never sorted to inclusions (Figures 2A and S2A).

In the Absence of Hsp104, Stress Foci are Inherited by Nascent Buds During Division, Abolishing Asymmetric Inheritance of Aggregates

Without Hsp104, aggregates in stress foci were now freely inherited by the buds (Figure 2A; Movies S7 and S8), and daughter/grand-daughter cells over several consecutive divisions (Figures 2B and S2A; Movies S9 and S10). Quantification of 200 budding events per strain revealed that multiple stress foci were aberrantly inherited by the daughter cell in 100% of the budding events (Figure 2C), whereas JUNQs and IPODs were retained in the mother cell in 100% of the budding events. Although some small aggregates, such as those formed by the proline-deletion variant of polyQ Huntingtin (Liu et al., 2011) have been shown to be asymmetrically partitioned in a polarisome- and Hsp104-dependent manner, in the absence of Hsp104 VHL and Ubc9^{ts} stress foci passed freely into the bud. On the other hand, even deletion of a critical polarisome component (Liu et al., 2010), Bud6, failed to disrupt JUNQ and IPOD inheritance by the mother cell (Figure 2C; data not shown for IPOD).

The Movement of JUNQs and IPODs into Daughter Cells is Constrained by their Attachment to Organelles

In their previous study, Zhou et al. (2011) had speculated, based on an ad hoc stochastic model of aggregate motion, that inheritance asymmetry might result from the sheer unlikelihood of

Please cite this article in press as: Spokoini et al., Confinement to Organelle-Associated Inclusion Structures Mediates Asymmetric Inheritance of Aggregated Protein in Budding Yeast, Cell Reports (2012), http://dx.doi.org/10.1016/j.celrep.2012.08.024

Cell PRESS
Open ACCESS

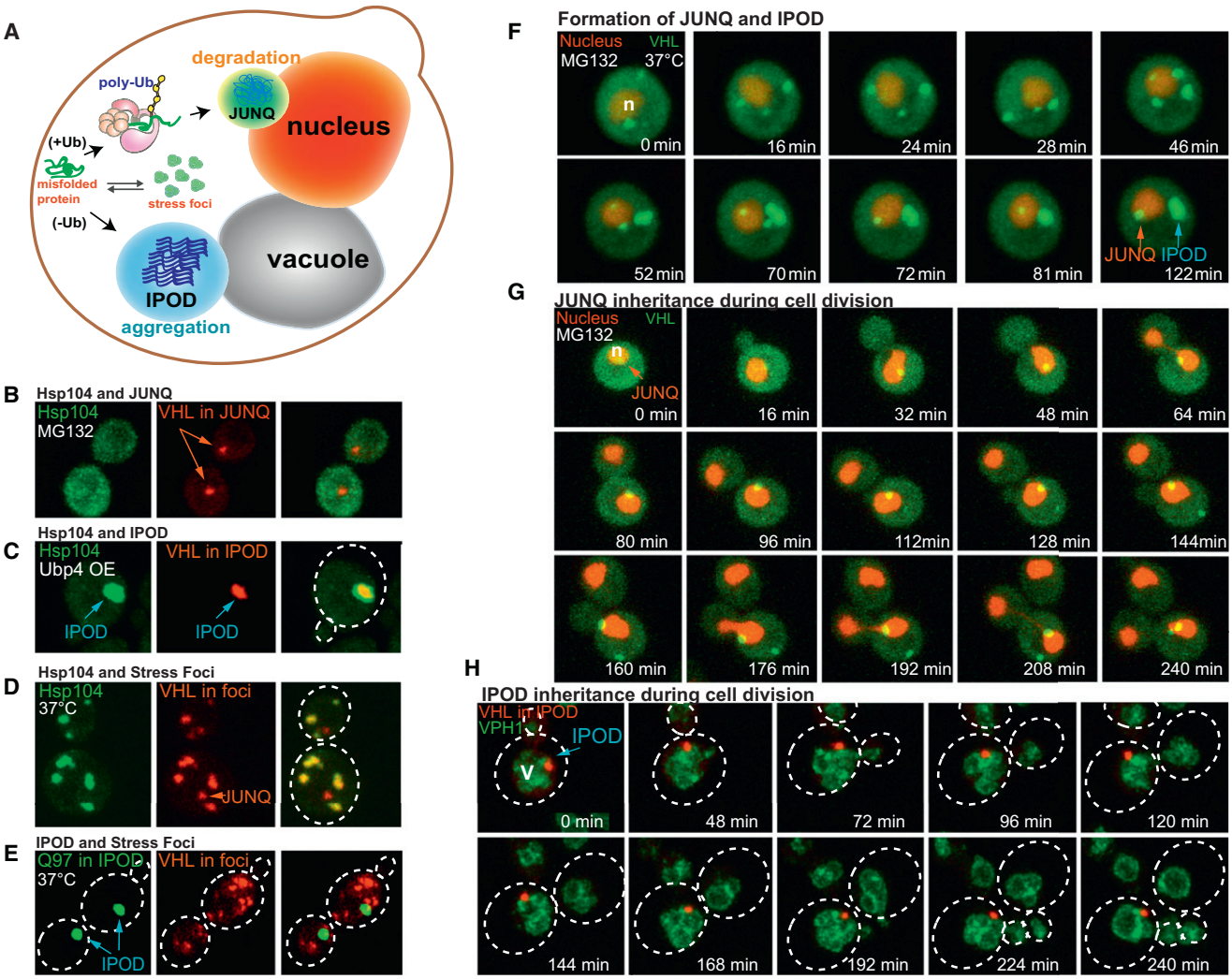

Figure 1. Aggregating Proteins are Partitioned to JUNQ and IPOD Inclusions, which are Asymmetrically Inherited During Budding

(A) Model: following misfolding or heat stress, aggregating proteins localize to proteostatic stress foci. They are then cleared from the cell or are processed into two compartments: (1) the JUNQ, which is attached to the nucleus and (2) the IPOD, which is attached to the vacuole.

(B) Blocking quality control-associated proteasomal degradation leads to the accumulation of misfolded VHL-ChFP (red) in the JUNQ, which does not colocalize with Hsp104-GFP (green). Proteasome was inhibited by adding 80 mM MG132 to yeast media. See also Movies S1 and S2.

(C) Hsp104-GFP (green) colocalizes at the IPOD with insoluble ChFP-VHL (red) when constitutively misfolded VHL is deubiquitinated via the overexpression of Ubp4 (also see Kaganovich et al., 2008).

(D) Upon temperature shift to 37°C, the misfolded VHL (red) forms proteostatic stress foci that are bound by Hsp104-GFP (green). VHL expression was shut off by addition of 2% glucose before temperature shift, as in all experiments. The JUNQ is also visible here and does not colocalize with Hsp104. See also Movie S3.

(E) Stress foci are distinct from IPODs. Here the IPOD is visualized with polyglutamine HttQ97-GFP, which forms amyloids. Stress foci are visualized with VHL-ChFP heat shocked at 37°C.

(F) Upon temperature shift to 37°C and proteasome inhibition with 80 mM MG132, the GFP-Ubc9^{ts} (green) stress foci are processed into JUNQ and IPOD inclusions. The nucleus is labeled by NLS-TFP (red). Three-dimensional images were acquired at 4 min intervals. See also Movie S4.

(G) The JUNQ, containing a soluble aggregate of GFP-VHL, is always asymmetrically inherited by the mother cell (200 cell divisions were scored). The nucleus is marked by NLS-TFP (red). Three-dimensional images were acquired at 4 min intervals. See also Movie S5.

(H) The IPOD, containing an insoluble aggregate of ChFP-VHL, is asymmetrically inherited by the mother cell. Over the course of cell budding, the IPOD remains attached to the vacuole, labeled with Vph1-GFP. Images were acquired at 4 min intervals. See also Movie S6.

See also Figure S1.

individual foci moving into the bud prior to division. Our data forced us to reject this hypothesis, first by establishing the specific and absolute asymmetry of inclusion inheritance, and second by showing that stress foci regularly diffuse into the bud if the absence of Hsp104 prevents their incorporation into inclusions. What remained was to identify a plausible alternative mechanism for the regulated retention of inclusions in mother cells. Toward this end, we noted that the diffusion of inclusions

Please cite this article in press as: Spokoini et al., Confinement to Organelle-Associated Inclusion Structures Mediates Asymmetric Inheritance of Aggregated Protein in Budding Yeast, Cell Reports (2012), http://dx.doi.org/10.1016/j.celrep.2012.08.024

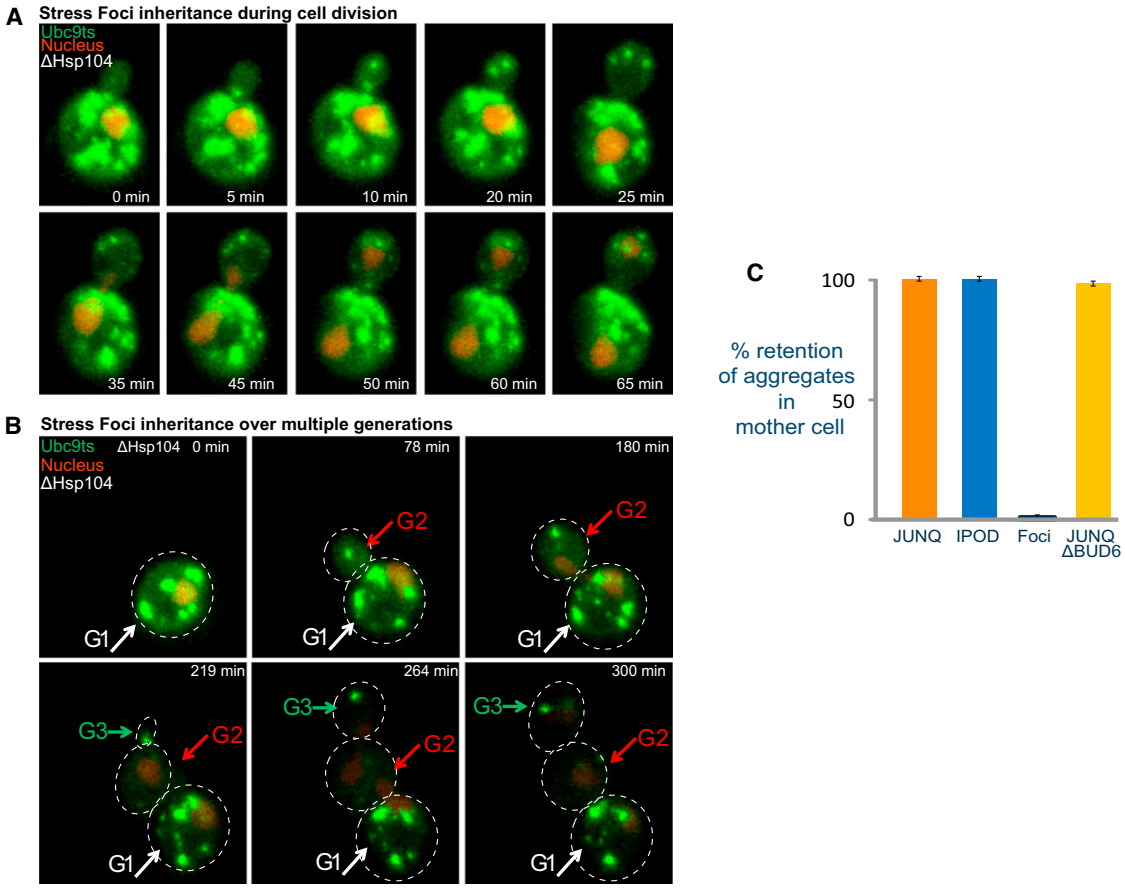

Figure 2. Inclusion-Unconfined Stress Foci are Symmetrically Inherited between Mother and Daughter Cells in the Absence of Hsp104

(A) Stress foci are freely inherited by the daughter cell in consecutive divisions. ΔHsp104 cells were transiently heat shocked (42°C, 45 min) to trigger protein aggregation. Upon recovery at 30°C, GFP-Ubc9^{ts} stress foci were followed. The nucleus is labeled by NLS-TFP (red). See also Movies S7, S8, and S9.

(B) Stress foci are freely inherited by daughter/grand-daughter cells. ΔHsp104 cells were transiently heat shocked (42°C, 45 min) to trigger protein aggregation. Upon recovery at 30°C, GFP-Ubc9^{ts} stress foci in mother and daughter cells were followed. The nucleus is labeled by NLS-TFP (red). See also Movie S10.

(C) Quantification of asymmetrical inheritance of different kinds of VHL aggregates during cytokinesis. Juxtanuclear quality control compartments and IPODs were retained in the mother cell in 100% of the budding events, whereas several stress foci were inherited by the daughter cell in 100% of the budding events in ΔHsp104 cells. All cells were transiently heat shocked (42°C, 45 min) to trigger protein aggregation. Upon recovery at 30°C, GFP-Ubc9^{ts} or GFP-VHL stress foci in mother and daughter cells were followed. N = 100–200 cells, error bars represent SE.

See also Figure S2.

into daughter cells appears to be constrained by their association with organelles—the vacuole in the case of the IPOD and the nucleus in the case of the JUNQ (Figures 3A and 3B; Movies S11, S12, and S13). The IPOD can always be observed colocalized with the vacuole, and diffraction-limited 3D structured illumination microscopy (SIM), which resolves to below 100 nm, demonstrated that the two structures are in contact (Figures 3E and S3B for intensity profile). This supports previous electron microscopy (EM) studies (Kaganovich et al., 2008; Tyedmers et al., 2010b) showing direct contact between the IPOD and the vacuole. Furthermore, the IPOD colocalizes with the Cvt19 protein, which has previously been shown to be associated with the vacuole at the preautophogosomal structure (Shintani and Klionsky, 2004; Figure S3A). The JUNQ, on the other hand, is confined to the surface of the nucleus. Three-dimensional confocal imaging demonstrated that the JUNQ forms in a visible "pocket" in the nuclear membrane (Figure 3D). These data are in agreement with previous 3D imaging and EM studies (Kaganovich et al., 2008). We therefore undertook to consider a simple explanation for the phenomenon of asymmetric inheritance of these aggregates: that their movement and inheritance is constrained by sequestration in organelle-associated inclusions.

To investigate this possibility, we examined the association between the IPOD and the vacuole by continuous acquisition (z stack every 5 s) 4D imaging of yeast cells. We observed that the movement of the inclusion in 3D corresponds perfectly with the vacuolar membrane (Figure 3A; Movie S11). Similarly, we generated 4D movies of the JUNQ and the nucleus. The path of the JUNQ clearly follows a trajectory along the surface of the nucleus (Figure 3B; Movies S12 and S13, side view). We monitored the inclusions and their organelles for periods of up to t = 90 min (e.g., Movies S6 and S12), and found that the

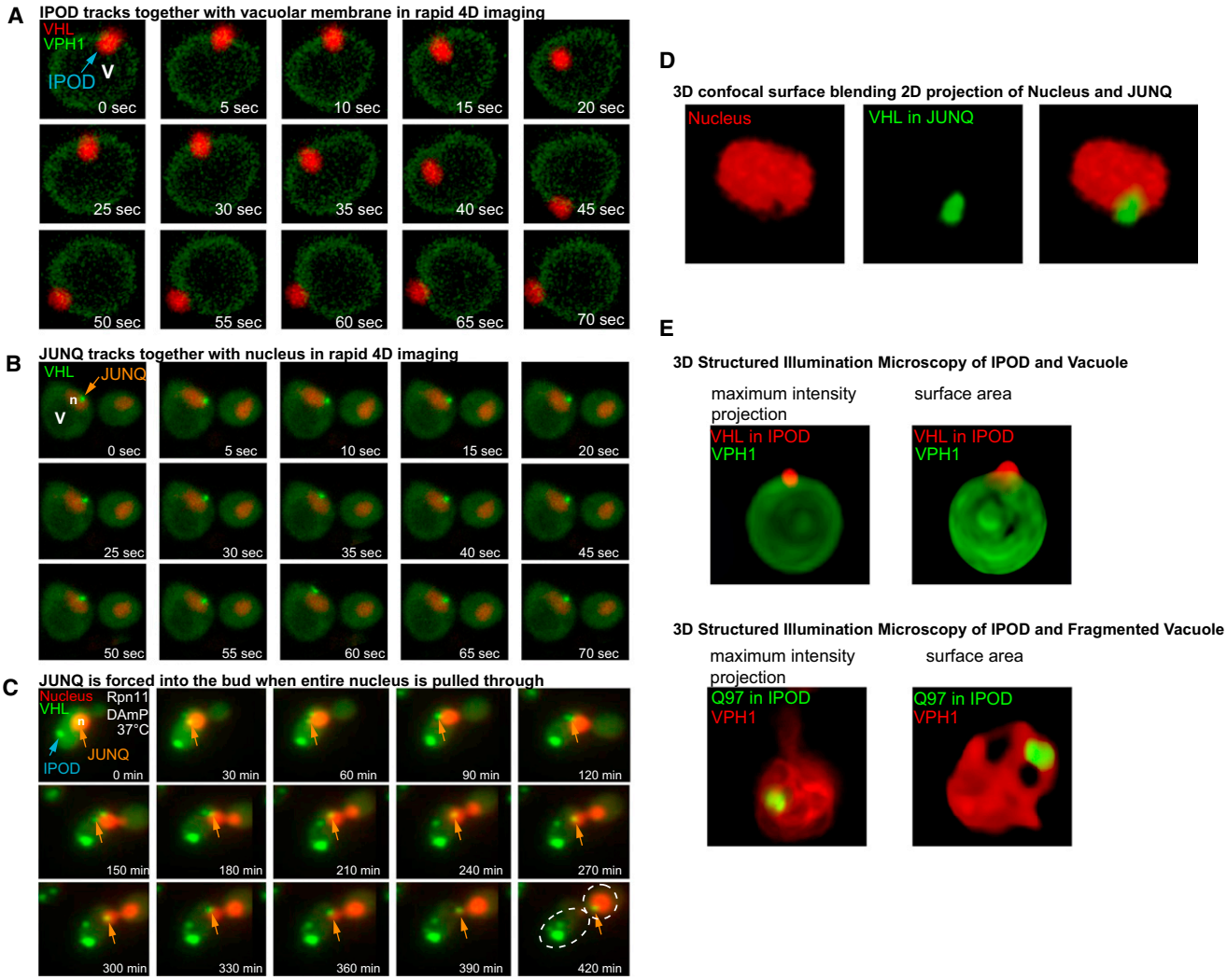

Figure 3. The Movement of Inclusions in the Cell is Determined by Their Confinement to the Surface of Organelles

(A) The IPOD, containing an insoluble aggregate of ChFP-VHL, moves along the surface of the vacuole. Vph1, a subunit of the vacuolar ATPase, is endogenously tagged with GFP (green). Three-dimensional images were acquired at 5 s intervals. See also Movie S11.

(B) The JUNQ, containing a soluble aggregate of GFP-VHL, moves along the surface of the nucleus, labeled by NLS-TFP (red; Kaganovich et al., 2008). Reduced proteasome activity (Rpn11-DAmP strain) leads to VHL accumulation in the JUNQ. Three-dimesional images were acquired at 5 s intervals. See also Movies S12 and S13 for side view.

(C) Mitotic arrest, caused by heat shock at 37°C in the rpn11-DAmP proteasome-inhibited background leads to aberrant inheritance of the JUNQ inclusion. Since sister-chromatid separation is blocked, the entire nucleus is pulled through to the daughter cell, together with the JUNQ. The JUNQ is visualized via a soluble aggregate of GFP-VHL; the nucleus is labeled by NLS-TFP (red). See also Movie S14.

(D) The JUNQ is localized to a "pocket" in the outer-nuclear membrane. A 3D confocal reconstruction is shown.

(E) Structured illumination microscopy shows diffraction-limited proximity (within 100 nm) between the vacuolar membrane and the IPOD. Reagents were used as above. Left panels show maximum intensity projections and right panels show surface blending. Upper panels are of a whole vacuole and lower panels show a fragmented vacuole.

See also Figure S3.

inclusions remained localized to their organellar surfaces without interruption. To quantify the significance of these results, we estimated the likelihood of a freely diffusing particle remaining in a one-dimensional interval roughly L = 0.5 microns in length with a reflecting right boundary (corresponding to the organellar surface) and an absorbing left one (corresponding to the rest of the cell). For this purpose, we assumed the diffusion constant employed in the model of Zhou et al. (2011) (0.0005 square microns per s), obtaining a p value estimate of $p \sim \exp[-tD\pi^2/4L^2] = 10^{-12}$. From this, we concluded that the observed movement of both inclusions cannot be accounted for by a random walk in all directions, and rather must be constrained in such a way that the inclusions remain confined to organellar surfaces by some means of attachment. Thus, the seemingly random

Please cite this article in press as: Spokoini et al., Confinement to Organelle-Associated Inclusion Structures Mediates Asymmetric Inheritance of Aggregated Protein in Budding Yeast, Cell Reports (2012), http://dx.doi.org/10.1016/j.celrep.2012.08.024

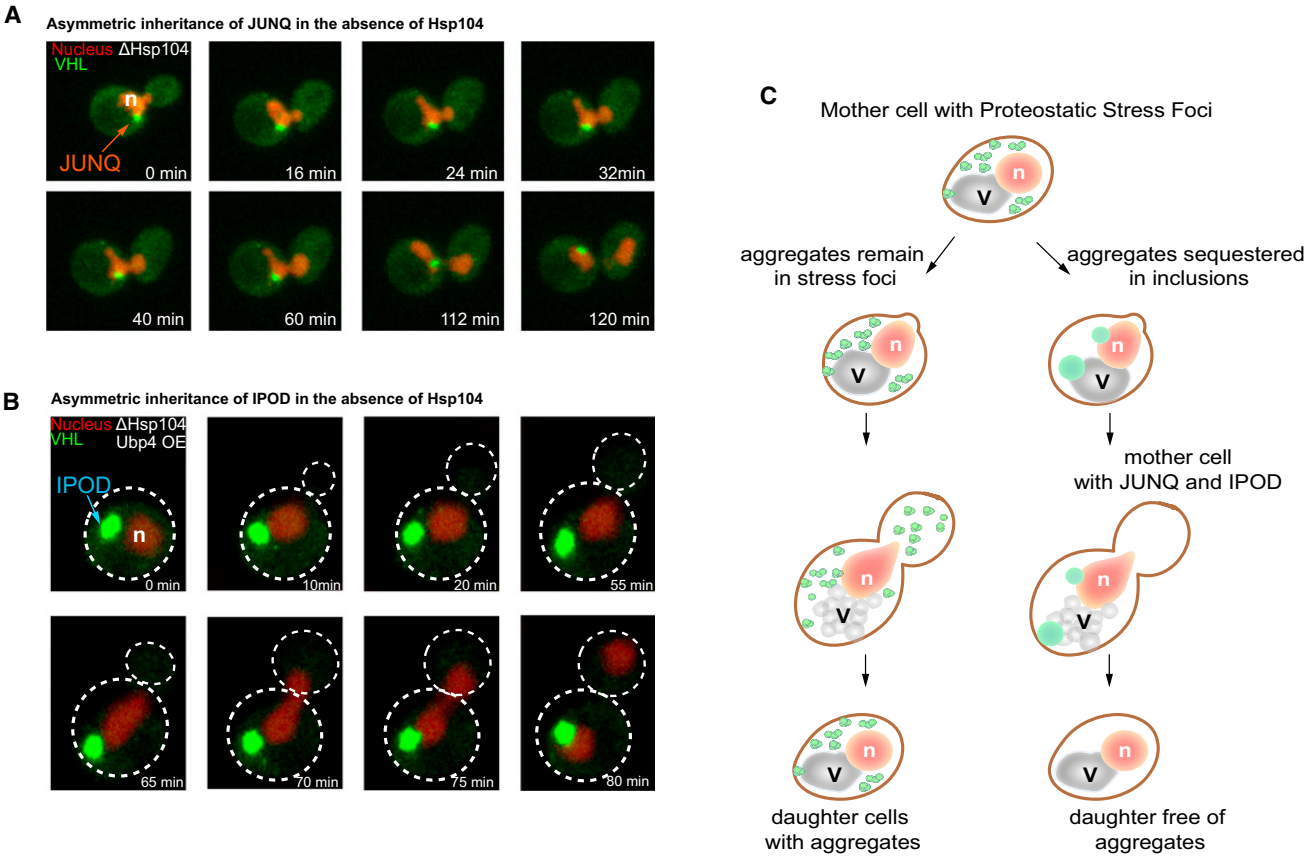

Figure 4. In the Absence of Hsp104, Delivery or Aggregates to JUNQ or IPOD is Sufficient for Their Asymmetric Retention in the Mother Cell

(A) VHL (green) localizes to the JUNQ, in the absence of heat shock and Hsp104. These JUNQs are asymmetrically inherited by the mother cells during budding. The nucleus is labeled by NLS-TFP (red).

(B) Targeting misfolded VHL (green) into an IPOD, by blocking its ubiquitination also restores asymmetrical inheritance to ΔHsp104 cells. The nucleus is labeled by NLS-TFP (red). The Ubp4 is overexpressed to block VHL ubiquitination. See also Movie S15.

(C) Model of asymmetric inheritance: Attachment to organelles ensures retention in the mother cell during budding. Nucleus-bound JUNQs and Vacuole-bound IPODs, are retained in the mother cell. Unconfined stress foci lacking Hsp104 are freely inherited by the daughter cell.

component of the trajectory with which the JUNQ and IPOD move within the cell is arguably the aspect of their motion that is least relevant to asymmetric inheritance. Instead, it is much more plausible that aggregate inheritance is determined by the asymmetry of organelle inheritance during the budding event.

Finally, in order to demonstrate that asymmetric retention of inclusions is not a categorical consequence of the inability of inclusions to pass through the bud neck, we picked a condition under which nuclear division during budding is disrupted. We observed the inheritance of the JUNQ in cells with poorly functioning proteasomes (rpn11-DAmP strain; Breslow et al., 2008) at 37°C. Since there is not enough proteasome activity in this strain at high temperatures to allow for sister-chromatid separation, the cells are unable to divide the nucleus and in some cases, the entire nucleus is pulled through to the daughter cell. Only in this case, when the entire nuclear structure was pulled through, did we observe aberrant inheritance of the JUNQ by the daughter cell (Figure 3C; Movie S14). This exception proves the rule: aggregates in the JUNQ are actively retained in mother cells through a regulated process that ensures asymmetric segregation, and in this rare case breaks down only because tethering to the nuclear structure forces aberrant inheritance by the daughter cell. These data suggest that by confining inclusions to organelles, cells are able to regulate their localization and movement during division.

Aggregates in JUNQ and IPOD are Asymmetrically Inherited even in the Absence of Hsp104

We noticed that Hsp104 is not required for delivering aggregates to JUNQ and IPOD per se, only to disaggregate stress foci, which without Hsp104 appear to be a trapped intermediate. Without heat shock, VHL aggregates were able to form JUNQs and IPODs (Figures 4A and 4B; in fact, we observed a greater incidence of spontaneous JUNQ formation [without proteasome inhibition] in the absence of Hsp104, likely due to a decrease in proteostasis buffering capacity). We exploited this fact to further validate our model. We asked whether forcing misfolded proteins into the IPOD by blocking their ubiquitination restores asymmetric inheritance of aggregates, even in Hsp104-deleted cells. In the absence of Hsp104, aggregates that are forced

into the IPOD by ubiquitin protease 4 (Ubp4) overexpression are once again completely retained in the mother cell (Figure 4B; Movie S15). The JUNQ was also completely retained in the mother cell over consecutive divisions without the presence of Hsp104. Thus, our data demonstrate that sequestration in a JUNQ or IPOD inclusion is sufficient for asymmetric inheritance of aggregates in yeast, even in the absence of Hsp104 (Figure 4C, model).

DISCUSSION

The accumulation of protein aggregates is often attributed to a decline of protein folding quality control functions in the cell (Nyström, 2011; Treusch et al., 2009; Winkler et al., 2012). Asymmetric aggregate inheritance has been proposed as a method of decreasing the aggregation load on a nascent cell, by partitioning aggregates to a specific lineage during division (Erjavec and Nyström, 2007; Liu et al., 2010, 2011; Nyström, 2011). Previous studies have demonstrated that aggregates of carbonylated proteins, colocalizing with Hsp104, are asymmetrically partitioned to the mother cell in budding yeast (Erjavec et al., 2007; Erjavec and Nyström, 2007). Damage to the actin cytoskeleton, whether direct or via deletion of the Sir2 deacetylase, as well as deletion of Hsp104, disrupted this asymmetry (Erjavec and Nyström, 2007). Remarkably, the disruption of asymmetric aggregate partitioning observed in the genetic deletions of Sir2 and Hsp104 coincided with a shorter replicative life span for the emerging daughter cells (Erjavec et al., 2007). It was hypothesized that the actin cytoskeleton plays a role in delivering aggregates to specific locations in the mother cell, thus preventing them from contaminating the bud, though other studies proposed a stochastic model of asymmetric inheritance over time(Liu et al., 2010, 2011; Zhou et al., 2011).

In this study, we use model misfolded proteins VHL and Ubc9^{ts} to demonstrate that Hsp104-mediated disaggregation of transient stress foci, and the delivery of aggregates to JUNQ and IPOD inclusions (depicted schematically in Figure 1A), is required for asymmetric inheritance of these aggregates. Aggregates that remain in stress foci in the absence of Hsp104 and are not retained in inclusions freely pass into the bud and are inherited by emerging generations of yeast. We therefore suggest a mechanism for ensuring asymmetric inheritance: sequestering aggregates in organelle-attached inclusions marks them for retention in the mother cell. Confinement of the JUNQ to the nucleus and the IPOD to the vacuole (Figure 4C) determines their asymmetrical inheritance. It is important to note that Hsp104 is not essential for the formation of JUNQ and IPOD inclusions (Figures 4A and 4B). Hence, it would appear that it is the disaggregase activity of Hsp104 (as opposed to its aggregase activity; Shorter and Lindquist, 2004, 2006; Winkler et al., 2012) that is required for the processing of stress foci into inclusions.

These results may help explain why the Hsp104 expression level is a predictor of yeast life span (Erjavec et al., 2007; Xie et al., 2012), and why overexpression of Hsp104 suppresses the Sir2 shortened life-span phenotype (Erjavec et al., 2007). Without disaggregation by Hsp104, damaged proteins cannot be sequestered in inclusions and therefore propagate through the generations, contaminating the emerging population of yeast.

In a previous study carried out by Zhou et al. (2011) it was suggested that asymmetric segregation arises as a simple consequence of how protein aggregates "anomalously diffuse" in the boundary conditions set by the size of the bud neck through which aggregates must pass in order to be inherited by the daughter. Our findings confound this proposal by demonstrating the ease with which stress foci may diffuse into the bud in the absence of Hsp104.

Intriguingly, our model also offers an easy explanation for the so-called "anomalous" diffusion reported by the authors in their study, in which aggregates were often observed to achieve mean-squared displacements from their starting positions that had a wide distribution of different power-law dependences on time. The authors referred to superlinear scaling as "superdiffusion" and sublinear scaling as "confinement"; however, they did not establish an explanation for either phenomenon. Our model of inclusion confinement on organellar surfaces suggests a possible mechanism for superdiffusion, insofar as an attachment to a large body like the nucleus or vacuole would couple an inclusion to shocks and stresses happening on the scale of the entire cell. In Movie S11, for example, the occasional sharp, sudden, nondiffusive jumps of the IPOD are coupled to the motion of the vacuole in a way that is highly suggestive of large scale intracellular rearrangements; however, this matter deserves further investigation.

The sublinear, "confinement"-type scaling Zhou et al. (2011) observed meanwhile has a natural explanation in the constraints placed on aggregate motions by membrane surfaces. Let us begin by considering physical intuition for the instructive case of a random walk on a sphere (such as the quasi-spherical nucleus or vacuole): over short times, the walk should traverse distances small compared to the radius of the sphere, and the scaling of mean square displacement (MSD) projected into the plane should be indistinguishable from that of a free random walk in a flat plane and should therefore be linear (Figure S3C). However, as time goes on, the random walk begins to experience the curvature of the sphere and ultimately runs up against an upper bound on how far away it can get from its starting point. The result is that the slope of MSD should hook downward with time, leading to an overall sublinear scaling at intermediate times.

This argument may be made rigorous by solving the rotational diffusion equation for the probability density $f(\theta, t)$

$$\dot{f} = D_r \nabla_\theta^2 f$$

with the initial condition of $f(\theta, 0) = \delta(\theta)$. (Here we have integrated out the irrelevant azimuthal angular variable ϕ). The solution may be written as

$$f(\cos\theta, t) = \frac{1}{4\pi} + \sum_{l=1}^{\infty} C_l P_l(\cos\theta) e^{-D_r l(l+1)t}$$

where C_l are positive constants and P_l are the Legendre polynomials. In the Extended Discussion, we show that the MSD

averaged uniformly over all possible two-dimensional (2D) projection planes may be expressed as

$$MSD(t) = \int d(\cos\theta) f(\cos\theta, t)[AP_0(\cos\theta) - BP_1(\cos\theta)]$$

where A and B are positive constants. Because of the orthogonality of the Legendre polynomials P_l, we therefore immediately obtain the exact result

$$MSD(t) = C\left(1 - e^{-2D_r t}\right)$$

where C is a positive constant. This type of sublinear time dependence is indistinguishable from the "anomalous" diffusive behavior previously reported.

A key point here is that both stress foci and inclusions might be expected to exhibit this type of behavior. To whatever degree diffusive motion was hampered by the presence of confining membrane surfaces (whether for an aggregate sandwiched in the 1–2 micron thick space between the vacuole and the plasma membrane, as in the case of stress foci, or one confined to the surface of the nucleus or vacuole, as in the case of an inclusion), this confinement would have measurable consequences in the sublinear scaling of MSD. Strikingly, when Zhou et al. (2011) assigned power-law exponents to the sublinear MSDs of so-called "aged" aggregates, i.e., IPOD inclusions, the exponents were near the extreme low end of the spectrum they observed in the diverse aggregate population as a whole, indicating that IPODs were atypically strongly confined (compared to stress foci). Indeed, it was only when the authors assumed this extremely high degree of confinement in their model of aggregate segregation that they were able to make their analytical model consistent with the extreme asymmetry observed in vivo. Thus, our model of membrane-based aggregate confinement is not only consistent with the data of Zhou et al. (2011) it also helps to clarify their own analysis of it.

It is still not clear what role actin cables play in delivery of aggregates to inclusions. The actin cytoskeleton is required for the maintenance of asymmetry and for inclusion formation. One possibility is that aggregates are transported by unknown machinery, along actin cables away from the daughter cells. Without knowing the machinery that links aggregate to actin cable, it is difficult to discount the possibility that a native actin cytoskeleton is required for the proper transport and diffusion of other elements in the cytosol, that ensure proper delivery of aggregates to inclusions. The data presented here highlight the importance of aggregate compartmentalization to protein folding quality control and aging and argue strongly for a factor-dependent model of asymmetric inheritance. Our model opens up an important direction in the study of aging in unicellular organisms and higher eukaryotes.

EXPERIMENTAL PROCEDURES

Yeast Strains and Materials

Yeast media preparation, growth, and yeast transformations were performed according to standard protocols as in (Kaganovich et al., 2008). von Hippel-Lindau protein, fused to GFP or mCherry fluorescent protein (ChFP) to facilitate detection, was expressed under the control of a galactose-regulated promoter (Gal1p). The strains were grown to OD600 0.8 in synthetic media containing 2% raffinose for 72 hr, diluted to OD600 0.2 in 2% galactose-containing media, and grown for 8 hr. To shut-off expression galactose-containing media was replaced with synthetic media supplemented with 2% glucose (SD). The genotypes of the strains and plasmids used in this study are summarized in Tables 1 and 2.

Table 1. Yeast Strains used in this Study

Name	Genotype	Source
BY4741	*MATa his3Δ1 leu2 Δ 0 met15 Δ 0 ura3 Δ 0*	Brachmann et al., 1998
RPN11 DAmP	*MATa his3Δ1 leu2 Δ 0 met15 Δ 0 ura3 Δ 0 RPN11Δ::kanMX4*	Schuldiner et al., 2005
VPH1-GFP	*MATa VPH1-GFP:HIS3 leu2Δ0 met15 Δ0 ura3 Δ0*	Huh et al., 2003
HSP104-GFP	*MATa HSP104-GFP:HIS3 leu2Δ0 met15 Δ0 ura3 Δ0*	Huh et al., 2003
ΔHSP104	*MATa his3Δ1 leu2 Δ 0 met15 Δ 0 ura3 Δ 0 HSP104Δ::kanMX4*	Winzeler et al., 1999
RPN11 DAmP ΔBUD6	*MATa his3Δ1 leu2 Δ 0 met15 Δ 0 ura3 Δ 0 RPN11Δ::kanMX4 BUD6Δ:: hphMX4*	this study
act1-133	*BY4741 act1-133::kanMX4*	Wertman et al., 1992
CVT19-GFP	*MATa CVT19-GFP:HIS3 leu2Δ0 met15 Δ0 ura3 Δ0*	Huh et al., 2003
VPH1-mCherry	*MATα leu2-3,112 ura3-52 his3-Δ200 trp1- Δ 901 lys2-801 suc2-Δ 9 VPH1-mCherry::TRP1*	Han and Emr, 2011

Fluorescent 3D Time Lapse: 4D Imaging

For time-lapse imaging, cells were seeded on concanavalin A-coated 384-well microscope plates (Matrical Bioscience) or 8-well chambered coverslips (Ibidi). Confocal 3D movies were acquired using a dual point-scanning Nikon A1R-si microscope equipped with a PInano Piezo stage (MCL), using a 60× PlanApo IR water objective NA 1.27, 0.3 micron slices, and 0.5% laser power (from 65 mW 488 laser and 50 mW 561 laser). Prior to imaging the point-spread function was visualized with 100 nm fluorescence beads in order to adjust the correction ring of the objective to the coverslip thickness. Images were acquired in resonant-scanning mode. z stacks were acquired every 5 s for 70 s or every 4 min for 70 min, with some exceptions. Each z series was acquired with 0.5 micron step size and 30 total steps. Image processing was performed using NIS-Elements software. Volume-view snapshots from movies are shown in Figures 1, 2, 3, 4, S1, S2, and S3 and the movies are shown in Movies S1, S2, S3, S4, S5, S6, S7, S8, S9, S10, S11, S12, S13, S14, and S15.

Long-Term Water Immersion Microscopy

Evaporative loss of water immersion fluid was countered by microfluidics. Briefly, a Chemyx Fusion 200 syringe pump was used to perfuse water at a rate of 10 μl/min through Tygon microtube with a 0.01 in internal diameter. Water formed a droplet at the end of the tubing and was pulled into the interface between the glass coverslip and the objective by capillary forces. This design permits water immersion microscopy for over 24 hr at 25°C.

Structured Illumination Microscopy Imaging

Cells were seeded on concanavalin A-coated Ibidi 35mm plates, with a 1.523 refractive index glass coverslip bottom (170 ± 10 μm thickness). Prior to imaging the point-spread function was visualized with 100 nm fluorescence

Table 2. Plasmids used in this Study

Name	Description	Source
pDK138	pESC-LEU-GAL1-CHFP-VHL	Kaganovich et al., 2008
pDK154	pESC-URA-GAL1-UBP4	Kaganovich et al., 2008
pDK259	pESC-URA- GAL1-GFP-Y68L (UBC9ts) GAL10-NLS-TFP	Kaganovich et al., 2008
pDK324	pESC-LEU-GAL1-GFP-VHL GAL10-NLS-TFP	Kaganovich et al., 2008
pMS108	pFA6-hphMX4	Longtine et al., 1998
pDK26	pESC-URA-Q97-GFP	Kaganovich et al., 2008

beads in order to adjust the correction ring of the objective to the coverslip thickness. For the images shown in Figure 3, a 60× water objective NA 1.27 was used. The raw data were examined carefully, and the optical grit pattern was clearly visible in all sets of images that were used. Images were reconstructed with NIS-Elements software.

SUPPLEMENTAL INFORMATION

Supplemental Information includes three figures and 15 movies and can be found with this article online at http://dx.doi.org/10.1016/j.celrep.2012.08.024.

LICENSING INFORMATION

ACKNOWLEDGMENTS

We thank members of the Kaganovich lab and Margaret Cunniff for valuable discussion of experiments and comments on the manuscript and Meytal Waiss for technical assistance. D.K. and R.S. are supported by an Israel Science Foundation grant (ISF 843/11), a grant from the Abisch-Frenkel Foundation, and a grant from the GIF, the German-Israeli Foundation for Scientific Research and Development (2267-2166.9/2010). M.S. and O.M. are supported by an ERC-StG-2010 260395 - ER Architecture grant.

Received: June 14, 2012
Revised: August 7, 2012
Accepted: August 21, 2012
Published online: September 27, 2012

REFERENCES

Aguilaniu, H., Gustafsson, L., Rigoulet, M., and Nyström, T. (2003). Asymmetric inheritance of oxidatively damaged proteins during cytokinesis. Science *299*, 1751–1753.

Brachmann, C.B., Davies, A., Cost, G.J., Caputo, E., Li, J., Hieter, P., and Boeke, J.D. (1998). Designer deletion strains derived from *Saccharomyces cerevisiae* S288C: a useful set of strains and plasmids for PCR-mediated gene disruption and other applications. Yeast *14*, 115–132.

Breslow, D.K., Cameron, D.M., Collins, S.R., Schuldiner, M., Stewart-Ornstein, J., Newman, H.W., Braun, S., Madhani, H.D., Krogan, N.J., and Weissman, J.S. (2008). A comprehensive strategy enabling high-resolution functional analysis of the yeast genome. Nat. Methods *5*, 711–718.

Delaney, J.R., Sutphin, G.L., Dulken, B., Sim, S., Kim, J.R., Robison, B., Schleit, J., Murakami, C.J., Carr, D., An, E.H., et al. (2011). Sir2 deletion prevents lifespan extension in 32 long-lived mutants. Aging Cell *10*, 1089–1091.

Erjavec, N., and Nyström, T. (2007). Sir2p-dependent protein segregation gives rise to a superior reactive oxygen species management in the progeny of *Saccharomyces cerevisiae*. Proc. Natl. Acad. Sci. USA *104*, 10877–10881.

Erjavec, N., Larsson, L., Grantham, J., and Nyström, T. (2007). Accelerated aging and failure to segregate damaged proteins in Sir2 mutants can be suppressed by overproducing the protein aggregation-remodeling factor Hsp104p. Genes Dev. *21*, 2410–2421.

Han, B.K., and Emr, S.D. (2011). Phosphoinositide [PI(3,5)P2] lipid-dependent regulation of the general transcriptional regulator Tup1. Genes Dev. *25*, 984–995.

Henderson, K.A., and Gottschling, D.E. (2008). A mother's sacrifice: what is she keeping for herself? Curr. Opin. Cell Biol. *20*, 723–728.

Huh, W.K., Falvo, J.V., Gerke, L.C., Carroll, A.S., Howson, R.W., Weissman, J.S., and O'Shea, E.K. (2003). Global analysis of protein localization in budding yeast. Nature *425*, 686–691.

Kaganovich, D., Kopito, R., and Frydman, J. (2008). Misfolded proteins partition between two distinct quality control compartments. Nature *454*, 1088–1095.

Liu, B., Larsson, L., Caballero, A., Hao, X., Oling, D., Grantham, J., and Nyström, T. (2010). The polarisome is required for segregation and retrograde transport of protein aggregates. Cell *140*, 257–267.

Liu, B., Larsson, L., Franssens, V., Hao, X., Hill, S.M., Andersson, V., Höglund, D., Song, J., Yang, X., Öling, D., et al. (2011). Segregation of protein aggregates involves actin and the polarity machinery. Cell *147*, 959–961.

Longtine, M.S., McKenzie, A., 3rd, Demarini, D.J., Shah, N.G., Wach, A., Brachat, A., Philippsen, P., and Pringle, J.R. (1998). Additional modules for versatile and economical PCR-based gene deletion and modification in *Saccharomyces cerevisiae*. Yeast *14*, 953–961.

Nyström, T. (2011). Spatial protein quality control and the evolution of lineage-specific ageing. Philos. Trans. R. Soc. Lond. B Biol. Sci. *366*, 71–75.

Rujano, M.A., Bosveld, F., Salomons, F.A., Dijk, F., van Waarde, M.A., van der Want, J.J., de Vos, R.A., Brunt, E.R., Sibon, O.C., and Kampinga, H.H. (2006). Polarised asymmetric inheritance of accumulated protein damage in higher eukaryotes. PLoS Biol. *4*, e417.

Schuldiner, M., Collins, S.R., Thompson, N.J., Denic, V., Bhamidipati, A., Punna, T., Ihmels, J., Andrews, B., Boone, C., Greenblatt, J.F., et al. (2005). Exploration of the function and organization of the yeast early secretory pathway through an epistatic miniarray profile. Cell *123*, 507–519.

Shintani, T., and Klionsky, D.J. (2004). Cargo proteins facilitate the formation of transport vesicles in the cytoplasm to vacuole targeting pathway. J. Biol. Chem. *279*, 29889–29894.

Shorter, J., and Lindquist, S. (2004). Hsp104 catalyzes formation and elimination of self-replicating Sup35 prion conformers. Science *304*, 1793–1797.

Shorter, J., and Lindquist, S. (2006). Destruction or potentiation of different prions catalyzed by similar Hsp104 remodeling activities. Mol. Cell *23*, 425–438.

Specht, S., Miller, S.B., Mogk, A., and Bukau, B. (2011). Hsp42 is required for sequestration of protein aggregates into deposition sites in *Saccharomyces cerevisiae*. J. Cell Biol. *195*, 617–629.

Treusch, S., Cyr, D.M., and Lindquist, S. (2009). Amyloid deposits: protection against toxic protein species? Cell Cycle *8*, 1668–1674.

Tyedmers, J., Mogk, A., and Bukau, B. (2010a). Cellular strategies for controlling protein aggregation. Nat. Rev. Mol. Cell Biol. *11*, 777–788.

Tyedmers, J., Treusch, S., Dong, J., McCaffery, J.M., Bevis, B., and Lindquist, S. (2010b). Prion induction involves an ancient system for the sequestration of aggregated proteins and heritable changes in prion fragmentation. Proc. Natl. Acad. Sci. USA *107*, 8633–8638.

Wertman, K.F., Drubin, D.G., and Botstein, D. (1992). Systematic mutational analysis of the yeast ACT1 gene. Genetics *132*, 337–350.

Winkler, J., Tyedmers, J., Bukau, B., and Mogk, A. (2012). Chaperone networks in protein disaggregation and prion propagation. J. Struct. Biol. *179*, 152–160.

Winzeler, E.A., Shoemaker, D.D., Astromoff, A., Liang, H., Anderson, K., Andre, B., Bangham, R., Benito, R., Boeke, J.D., Bussey, H., et al. (1999). Functional characterization of the *S. cerevisiae* genome by gene deletion and parallel analysis. Science *285*, 901–906.

Xie, Z., Zhang, Y., Zou, K., Brandman, O., Luo, C., Ouyang, Q., and Li, H. (2012). Molecular phenotyping of aging in single yeast cells using a novel microfluidic device. Aging Cell *11*, 599–606.

Zhou, C., Slaughter, B.D., Unruh, J.R., Eldakak, A., Rubinstein, B., and Li, R. (2011). Motility and segregation of Hsp104-associated protein aggregates in budding yeast. Cell *147*, 1186–1196.

Cell PRESS
Open ACCESS

EXTENDED DISCUSSION

Since Zhou et al. present their data in a two-D maximum-intensity projection of a three-D *z*-stack, we were spurred to ask the following question: what would we expect the data to look like if we tracked the two-D projection of the three-D random walk of an aggregate confined to the surface of a sphere of fixed radius?

Let us assume that the starting point for our walk is the ''north pole'' of a unit sphere centered on the *z*-axis, so that the initial position vector for the walk is the unit vector $\hat{\boldsymbol{z}}$. At some later time, the random walk will carry us to a new position on the unit sphere $\hat{\boldsymbol{v}}$ with some known probability density $f(\hat{\boldsymbol{v}})$, and we are interested to know the mean-squared length of the projection of the displacement vector $\hat{\boldsymbol{v}} - \hat{\boldsymbol{z}}$ into a plane of arbitrary unit normal vector $\hat{\boldsymbol{w}}$, averaged over all possible $\hat{\boldsymbol{w}}$. That is, we wish to calculate the mean-squared displacement (*MSD*)

$$MSD = \frac{1}{4\pi}\int d\Omega_{\hat{\boldsymbol{w}}} d\Omega_{\hat{\boldsymbol{v}}} f(\hat{\boldsymbol{v}}) \|\hat{\boldsymbol{v}} - \hat{\boldsymbol{z}} - [(\hat{\boldsymbol{v}} - \hat{\boldsymbol{z}})\cdot\hat{\boldsymbol{w}}]\hat{\boldsymbol{w}}\|^2$$

In order to do this, we note that

$$\|\hat{\boldsymbol{v}} - \hat{\boldsymbol{z}} - [(\hat{\boldsymbol{v}} - \hat{\boldsymbol{z}})\cdot\hat{\boldsymbol{w}}]\hat{\boldsymbol{w}}\|^2 = \|\hat{\boldsymbol{v}} - \hat{\boldsymbol{z}}\|^2 - [(\hat{\boldsymbol{v}} - \hat{\boldsymbol{z}})\cdot\hat{\boldsymbol{w}}]^2$$

and furthermore, that

$$\int d\Omega_{\hat{\boldsymbol{w}}} d\Omega_{\hat{\boldsymbol{v}}} f(\hat{\boldsymbol{v}}) [(\hat{\boldsymbol{v}} - \hat{\boldsymbol{z}})\cdot\hat{\boldsymbol{w}}]^2 = \int d\Omega_{\hat{\boldsymbol{v}}} f(\hat{\boldsymbol{v}}) \|\hat{\boldsymbol{v}} - \hat{\boldsymbol{z}}\|^2 \int d\Omega_{\hat{\boldsymbol{w}}} \left[\widehat{\hat{\boldsymbol{v}} - \hat{\boldsymbol{z}}}\cdot\hat{\boldsymbol{w}}\right]^2 \propto \int d\Omega_{\hat{\boldsymbol{v}}} f(\hat{\boldsymbol{v}}) \|\hat{\boldsymbol{v}} - \hat{\boldsymbol{z}}\|^2$$

Thus, the whole calculation may be written as

$$\begin{aligned}\int d\Omega_{\hat{\boldsymbol{w}}} d\Omega_{\hat{\boldsymbol{v}}} f(\hat{\boldsymbol{v}}) \|\hat{\boldsymbol{v}} - \hat{\boldsymbol{z}} - [(\hat{\boldsymbol{v}} - \hat{\boldsymbol{z}})\cdot\hat{\boldsymbol{w}}]\hat{\boldsymbol{w}}\|^2 \propto \int d\Omega_{\hat{\boldsymbol{v}}} f(\hat{\boldsymbol{v}}) \|\hat{\boldsymbol{v}} - \hat{\boldsymbol{z}}\|^2 &= \int d\Omega_{\hat{\boldsymbol{v}}} f(\hat{\boldsymbol{v}})(2 - 2\hat{\boldsymbol{v}}\cdot\hat{\boldsymbol{z}}) = A' - B' \int d(\cos\theta) f(\cos\theta)\cos\theta \\ &= \int d(\cos\theta) f(\cos\theta)[AP_0(\cos\theta) - BP_1(\cos\theta)]\end{aligned}$$

where the functions $P_l(\cos\theta)$ are Legendre polynomials.

Cell PRESS
Open ACCESS

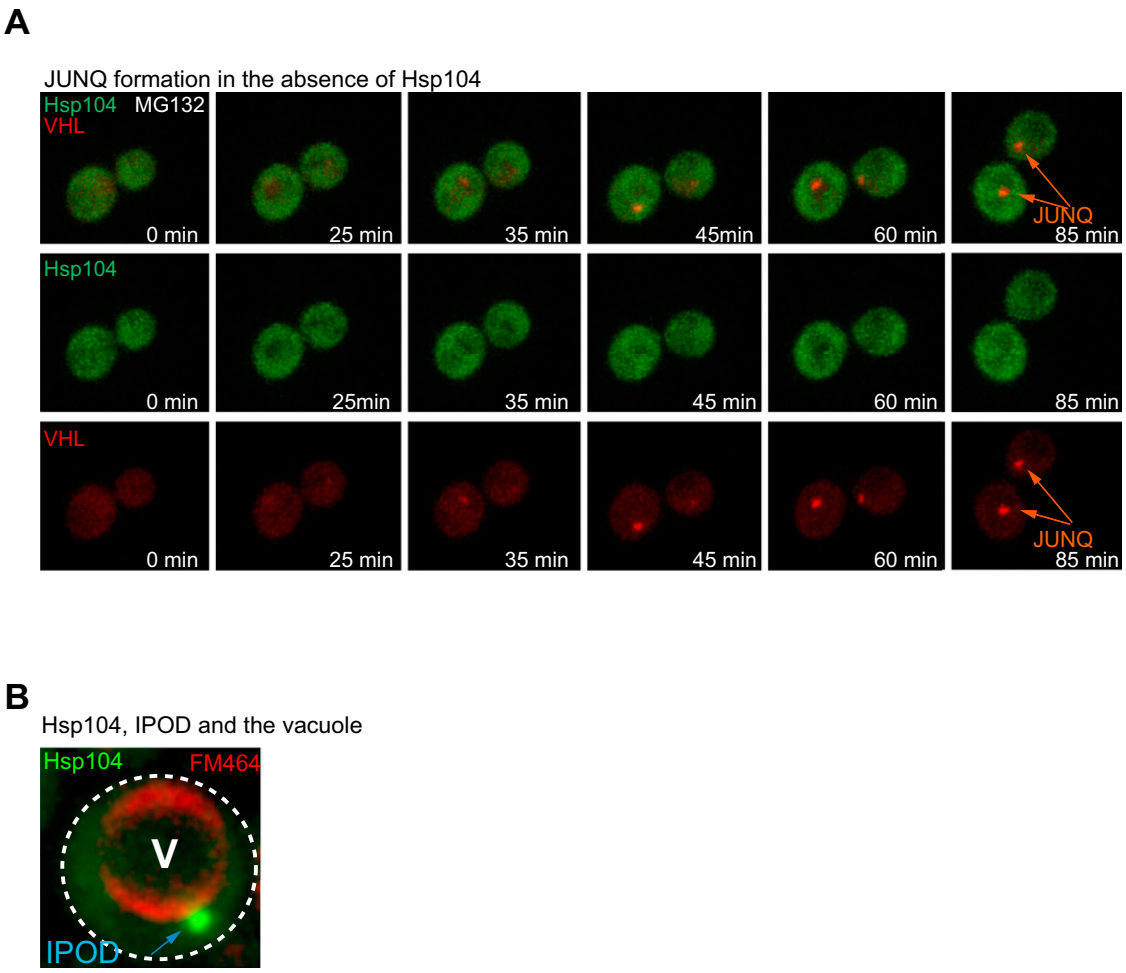

Figure S1. Hsp104 Colocalizes with IPOD, but not JUNQ Inclusions, Related to Figure 1

(A) Blocking quality control-associated proteasomal degradation leads to the accumulation of misfolded VHL-ChFP (red) in the JUNQ, which does not colocalize with Hsp104-GFP (green). Proteasome was inhibited by adding 80 mM MG132 to yeast media (also see Movies S1 and S2).

(B) Hsp104-GFP is localized at the IPOD inclusion (adjacent to the vacuole labeled by FM-464).

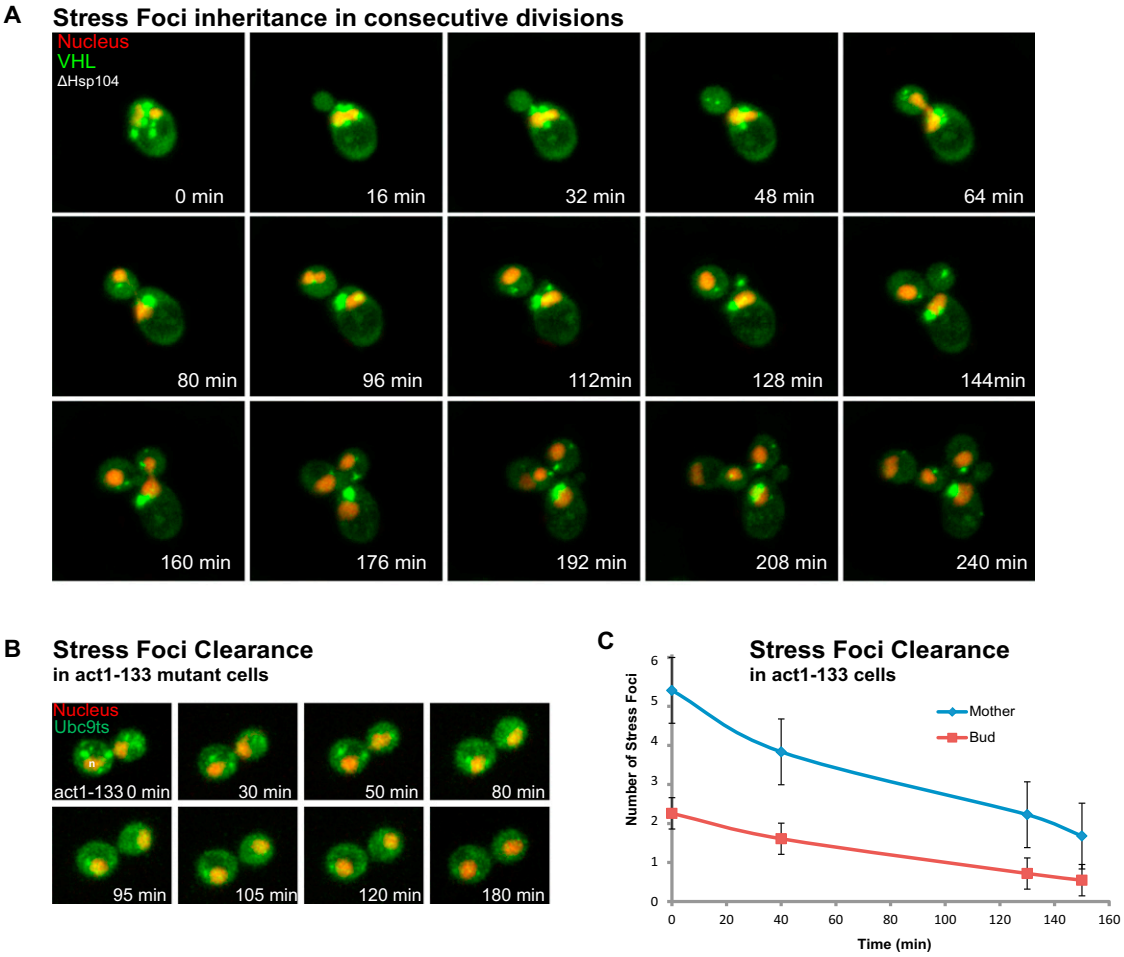

Figure S2. Stress Foci are Cleared by Hsp104 and are Passed On to Daugter Cells When not Cleared, Related to Figure 2

(A) Stress foci are freely inherited by the daughter cell in consecutive divisions. ΔHsp104 cells were transiently heat shocked (42°C, 45 min) to trigger protein aggregation. Upon recovery at 30°C, GFP-Ubc9^{ts} stress foci were followed. The nucleus is labeled by NLS-TFP (red; also see Movies S7, S8, and S9).

(B and C) Stress foci formed by Ubc9^{ts} are cleared on the time scale of a cell division in both mother and daughter cells upon shift from 42°C to 25°C. The act1-133 mutant was used to block budding, movement, and inclusion formation (Specht et al., 2011) following heat shock, in order to monitor stress foci disaggregation by Hsp104. Quantification is shown in (C) (n = 16 cells in which the nuclear furrow was still visible, error bars represent standard error). The quantification was done by carefully inspecting the entire cell in 3D volume view for presence of stress foci.

Cell PRESS
Open ACCESS

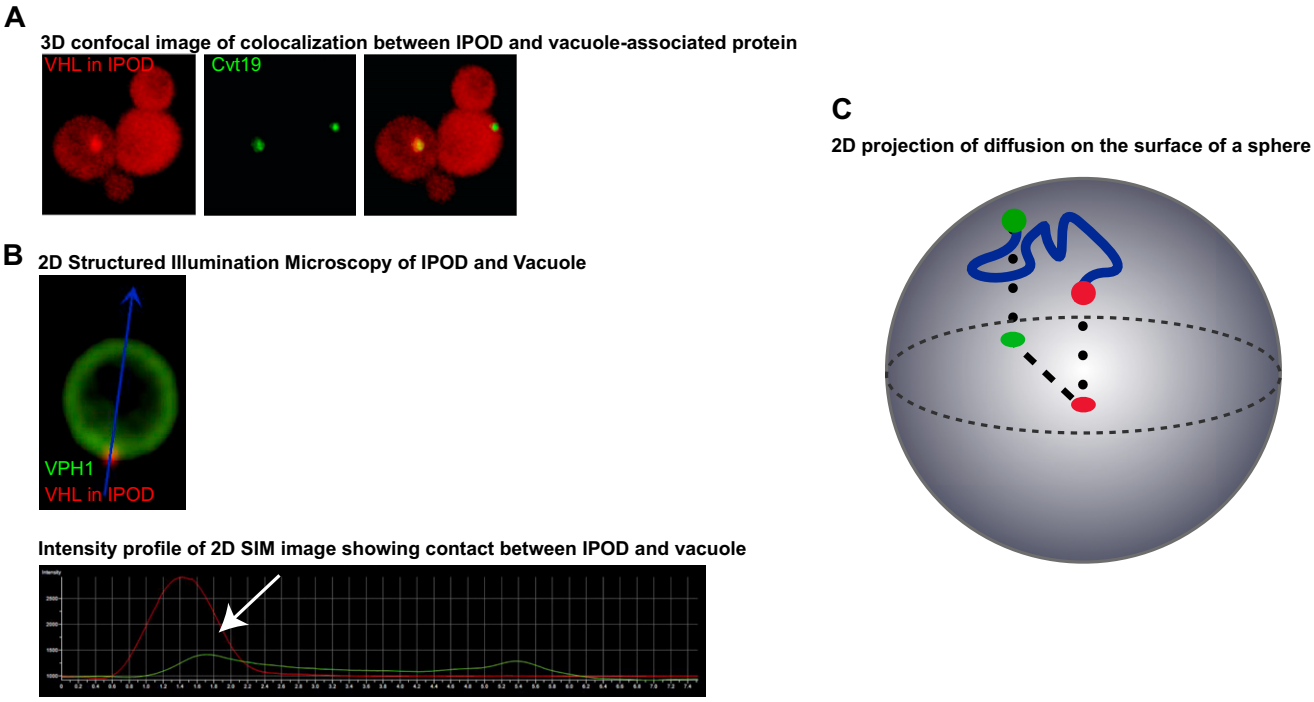

Figure S3. The IPOD is Attached to the Surface of the Vacuole, Related to Figure 3

(A) The IPOD (visualized by ChFP-VHL) colocalizes with Cvt19, which is part of the preautophagosomal structure and colocalizes with the vacuole.

(B) Intensity profile for IPOD-vacuole SIM image, showing a point of overlap at 100 nm resolution of the two structures.

(C) The displacement for diffusion constrained to the surface of a sphere, projected into a plane of arbitrary relative orientation.